Assessment of seismic performance of bridge pile foundation in liquefying soil using beam on Winkler foundation approach

Akihiro TAKAHASHI[1], Shunsuke TANIMOTO[1], Kazuyuki HAYASHI[1], Hideki SUGITA[1], Keiichi TAMURA[2], Mitsu OKAMURA[3], & Yumiko INOUE[4]

ABSTRACT

Detailed observations of damage to the pile foundations in liquefied soils revealed that the damage occurred not only at the pile heads but also near an interface between liquefied and non-liquefied soils due to large liquefied soil deformations and curvature demands at the interfaces. In practice a beam on Winkler foundation approach is believed to be a promising candidate for pile foundation performance assessment in large soil deformations. This paper demonstrates application of the beam on Winkler foundation approach to a pile foundation in liquefying soil by comparing the analysis results with centrifuge model test data.

1. INTRODUCTION

One of the major sources of earthquake-induced damage to pile foundations is liquefaction of saturated sandy soils. Detailed observations of damage to the pile foundations after the 1995 Kobe Earthquake revealed that the damage occurred at depths other than the pile heads, particularly near an interface between liquefied and non-liquefied soils due to large liquefied soil deformations and curvature demands at the interfaces (Tokimatsu & Asaka, 1998). This is a major cause of damage and is consequently a major concern both in research and design practice.

In practice a beam on Winkler foundation approach is believed to be a promising candidate for such a pile foundation performance assessment in large soil deformations and has already introduced in some of practical design codes in Japan (JSCE 2000). This method is a pseudo-static analysis of a pile foundation subjected to a superstructure inertial force and soil movement through Winkler springs that model soil-pile interaction (kinematic interaction).

Non-linear Winkler (p-y) springs that model lateral soil-pile interaction play a key role in this analysis. This paper firstly reports p-y curves directly measured at relatively strong surface layer overlying liquefied layer in centrifuge model tests. Based on this test results, the normalised p-y curve for the surface layer is modelled as an equivalent linear Winkler spring. A series of centrifuge model tests on a pile group in the liquefying soil is analysed by the pseudo-static beam on Winkler foundation approach using the examined spring for the surface layer and that recommended in the specifications for highway bridges (JRA 2002) for the other layers. In the analyses, scaling factor of p-y curves for liquefied soils to those for static drained loading is determined to fit the pile bending moment profiles to that measured in the centrifuge model tests.

[1] Earthquake Disaster Prevention Research Group, Public Works Research Institute, Japan

[2] Research Center for Disaster Risk Management, National Institute for Land and Infrastructure Management, Japan

[3] Dept of Civil & Environmental Engineering, Ehime University, Japan

[4] Dept of Civil & Environmental Engineering, Nagaoka University of Technology, Japan

2. DIRECT MEASUREMENT OF P-Y CURVES AT SURFACE LAYER

2.1 Test procedure and conditions

Direct measurement of the lateral resistance of a pile at the surface non-liquefiable layer during an earthquake was attempted in centrifuge model tests. Similar tests have been undertaken on an ordinary shaking table (Ono et al., 2003). The model setup used in this study is shown in Fig. 1. A laminar box used had inner size of 750mm in width, 380mm in breadth, and 500mm in height. Model piles equipped with load cells for direct pile lateral resistance measurement were placed at the centre of the laminar box as shown in Fig. 1. Since the tip and top cap of the model pile were fixed on the box base and the reaction frame, the model pile behaved as a very rigid pile. These piles were installed in loose Toyoura sand prepared by air pluviation. Higher viscosity fluid is usually used as pore fluid to avoid conflict with the scaling laws associated with the time of dynamic events and the seepage in centrifuge tests (Sakemi et al., 1995). Sand layers were saturated with a methyl-cellulose-base solution (Hiro-oka et al. 1995), which had a viscosity 25 times higher than that of water under a negative pressure of about 98kPa in a large tank by applying a vacuum. Ground water level and density for all the cases are listed in Table 1. Having prepared the model, the container was set on the shaking table mounted on the centrifuge. Shaking tests were undertaken at 25G centrifugal acceleration. Input motion was sinusoidal waves with a frequency of 30Hz, which is equivalent to 1.2Hz in the prototype scale, to the shaking table. Amplitude of input motion was varied with cycles to measure *p-y* relation covering wide range of relative displacement between soil and pile as shown in Fig. 2. During shaking, surface settlement, acceleration and excess pore water pressure in soil were measured at the locations shown in Fig. 1.

2.2 Determination of k_h for surface layer

All centrifuge test results presented in the following sections are in the prototype scale.

Figure 3 shows typical loops of relationship between the lateral resistance (p) and relative displacement between soil and pile (y) for Case 1-1. Secant subgrade reaction coefficient k_h normalised by σ_v'/D against y/D is plotted in Fig. 4, where σ_v'=effective overburden pressure, D=diameter of the pile and y=relative displacement between soil and pile. As expected (1) the larger relative displacement between soil and pile (y) and (2) the smaller soil density makes k_h smaller. Since a single non-dimensional linear curve can be sketched through the data points with reasonable confidence for each case when the data are plotted on logarithmic graph paper, they may be approximated by the following equation:

$$\frac{k_h D}{\sigma_v'} = A(y/D)^{-B} \tag{1}$$

where A and B are constants. Parameter A providing B=0.7 for all the cases is listed Table 2 and the broken line in Fig. 3 is a typical approximated curve. Probably parameter B is a material constant and A is a state parameter. The denser soil is, the larger parameter A is, which indicates that parameter A is a function of soil density.

3. PILE RESPONSE IN LIQUEFING SOIL

3.1 Test procedure and conditions

Centrifuge model tests were undertaken to examine dynamic soil-pile interaction in sandy ground having different configuration of liquefiable layer and overlying non-liquefiable layer. These results are utilised for assessment of applicability of the beam on Winkler foundation approach to a pile foundation in liquefying soil. The model setup used in this study is shown in Fig. 5. A strong box used had inner sizes of 800mm in width, 200mm in breadth, and 300mm in height. The model structure consisted of an aluminium footing weighing 4.2kg and 4 piles rigidly fixed to the footing. The pile spacing ratio s/D=5, as shown in Fig. 5. The piles were aluminium tubes having an outside diameter of 20mm, a thickness of 1mm, and a total length of 250mm below the footing bottom face. Strain gauges were instrumented inside one of the piles at 8 different levels. The piles were installed in three layers; (1) a bottom dense sand bearing stratum, (2) a saturated loose liquefiable sand layer, and (3) a top surface layer above ground water level. Test conditions for all the cases are listed in Table 3. The sand used was Toyoura sand and were prepared by air pluviation method to achieve the relative densities of 95% for the bottom bearing stratum and 27% for the middle liquefiable layer and the top surface layer. The bearing stratum thickness was 130mm and an embedded length of the pile into the bottom layer was 100mm. The bottom and middle layers were saturated with a methyl-cellulose-base solution having a viscosity 63 times higher than that of water. Shaking test was conducted under 63G by applying 20 sinusoidal waves motion with a frequency of 63Hz (1Hz in the prototype scale) and an amplitude of 32G (500gal in the prototype scale), shown in Fig. 6.

3.2 Pile foundation response in liquefying soil

Figure 7 shows time evolutions of relative horizontal displacement of ground at a shallow depth (1.6m below ground level) and the top of bearing stratum (GL-11m) to the model container bottom, together with those of excess pore water pressure ratio (L_U) above (P3) and below (P2) the boundary of bearing stratum and liquefiable layer. The relative horizontal ground displacements are calculated from outputs from the accelerometer at A5 (near surface), A2 (middle of the ground) and A17 (base input). The excess pore water pressure ratio is defined as a ratio of the excess pore water pressure to the effective overburden pressure before earthquake.

In all the cases, L_U at P3 (bottom of the liquefiable layer) reached one and liquefied at time t=10sec (7.5sec from the trigger of earthquake motion) and the amplitude of horizontal displacement near the ground surface since then. Regarding bearing stratum responses, L_U at the top of bearing stratum (P2) increased up to 0.8 during shaking and the amplitude of horizontal displacement below the boundary of bearing stratum and liquefiable layer gradually increased with time. These imply that the coefficient of subgrade reaction at the bearing stratum also gets smaller with shaking.

Time evolutions of relative horizontal displacement of ground surface and the footing to the bottom are plotted in Fig. 8, together with those of the horizontal footing acceleration. In all the cases, displacement of the footing was always larger than that of the ground surface. This fact indicates that the surface layer behaved as a passive resister.

Looking at the footing accelerations, the amplitude gradually increased with time in the case of the thinnest liquefiable layer (Case 2-6), while it decreased or kept constant in the other cases. This probably relates to change of natural frequency of the soil-pile-structure

system, i.e., decrease in subgrade reaction coefficient of soil layers. Figure 9 shows Fourier spectra of free vibration of the footing and shaking table just after shaking (t=30sec). The footing natural frequency before shaking was about 4.7Hz for all the cases, and it moved toward nil in the course of soil liquefaction during shaking. The footing natural frequencies just after shaking were about 0.5Hz for Case 2-3 and 2Hz for Case 2-6 (it was not clear for Case 2-4, though).

In the case without strong surface layer (Case 2-3), drastic softening of the liquefied layer and bearing stratum made the footing natural frequency smaller and well below the predominant frequency of the input motion (f_i), resulting in smaller acceleration response of the footing. In this course of event, the footing acceleration response once increased and then started decreasing when the footing natural frequency became less than f_i.

On the other hand, even though the footing natural frequency was pushed down by generation of excess pore water pressure in saturated soil layers in the case with thick non-liquefiable surface layer (Case 2-6), it remained higher than the input motion predominant frequency when shaking ceased. In this case, softening of the liquefied layer and bearing stratum was not enough to make the footing natural frequency smaller than f_i due to the strong and thick surface layer and merely got closer to f_i, i.e., the footing acceleration response continuously increased with time as shown in Fig. 8.

As these kinds of difference in footing response change due to liquefaction may heavily depend on an earthquake type (impact or vibration types) and its duration, these pose difficulties to application of the simple quasi-static analysis to assessment of seismic pile performance in liquefying soils.

4. ANALYSIS OF PILE RESPONSE IN LIQUEFYING SOIL USING BEAM ON WINKLER FOUNDATION APPROACH

4.1 Analysis procedure and conditions

Using the surface layer spring measured in Section 2 and the soil spring recommended in the specifications for road bridges (JRA 2002) for the other layers, centrifuge model tests on a pile group in the liquefied soil, described in the previous section, is analysed by the pseudo-static beam on Winkler foundation approach. Figure 10 illustrates the analytical model used. The vertical beam models the pile and the horizontal springs connecting the beam and supporting ground model soils. Rotation of the beam top corresponding to the pile top cap is restrained and that of the bottom end (pile tip) is not restrained. In the analyses, the inertial force is applied to the beam top as a horizontal load and the horizontal ground movement is imposed to the beam through the springs. Input soil displacement profile is calculated from the measured acceleration in the ground, neglecting accumulated permanent displacements.

Since the analyses presented here are performed at a snapshot in time, selection of the target time in an earthquake is a crucial factor, i.e., (1) critical situation of the target foundation and (2) main concern of the analysis have to be clarified. Based on these considerations, the superstructure inertial force and the soil displacement profile have to be estimated in a design situation. The former would require that taking account of effects of liquefaction on dynamic response of soil-pile-structure system (e.g. Sato et al., 2001, Kobayashi & Tamura, 2002) and the latter would require a site response analysis or an empirical correlation between in-situ logging data and estimated soil shear strain (e.g. Toki-

matsu & Asaka, 1998). Since these are challenging tasks and there are full of difficulties for reliable quantitative estimation of these in liquefying soils, these are outside the scope of this paper.

As our main concern in this section is response of the pile foundation in liquefied soil, the time when the liquefiable sand layer fully liquefied and a peak inertial load acted on the pile head (around t=19.5sec) is selected and measured data at the time are input in the analysis to demonstrate performance of the analysis method. Scaling factor of p-y curves for liquefied soil, D_E, to that for static drained loading is firstly determined to fit the pile bending moment profiles to that measured in the centrifuge model tests. Using this scaling factor for liquefied layer, analyses on pile in the liquefying soil overlaid by the non-liquefiable surface layer are performed. In these analyses, since the coefficient of subgrade reaction at the bearing stratum also gets smaller with shaking as mentioned in the previous section, this is taken into account by introducing scaling factor proposed by Tokimatsu (2003):

$$k_h = k_{hr}(1 - L_U)^{\alpha} \tag{2}$$

where k_{hr}= coefficient of subgrade reation at L_U=0 and α=0.5 (Tokimatsu's recommended range for α is 0.5 to 1). In the calculation excess pore water pressures measured at the array far from the pile foundation (P1 to P5 in Fig. 6) are used.

4.2 Determination of scaling factor for liquefied layer

In order to determine an appropriate scaling factor for the subgrade reaction coefficient for liquefied soil, analyses are made for the case without non-liquefiable surface layer (Case 2-3). In this calculation, the scaling factor D_E is varied from 1/1000 to 1/10. Pile bending moment distributions and displacement profiles of soil and pile are plotted in Fig. 11. Within the range of D_E used in the calculation, no remarkable difference can be seen in the bending moment distributions and the analysis results are comparable to the test results irrespective of D_E. However, D_E=1/10 is selected as the scaling factor for the liquefied layer and is used in the following calculations since the larger D_E, i.e., D_E=1/10 gives slightly better results.

4.3 Response of pile in liquefying soil overlaid by non-liquefiable surface layer

Figure 12 shows calculated bending moment distributions of the pile and displacement profiles of soil and pile for the cases with the non-liquefiable surface layer (Cases 2-4 & 2-6). In both the cases, although the calculated maximum pile bending moment in the bearing stratum is almost double of the observed, they can capture the observation in the other layers, i.e., the pile bending moment in the middle liquefiable layer and top non-liquefiable surface layer. Considering the fact that D_E for the liquefiable layer is insensitive to the pile bending moment profile as pointed out in the previous subsection, these results proves that estimation of the coefficient of subgrade reaction for the non-liquefiable surface layer in the separate special tests described in Section 2 is nicely done.

The larger calculated pile bending moment in the bearing stratum is probably due to the stiffer subgrade reaction in the bearing stratum, and results in the smaller horizontal displacement of the pile top cap. There are two possible reasons for this; (1) wrong determination of the α value in Equation 2, and (2) underestimation of excess pore water pres-

sure used for the k_h scaling factor calculation.

The α of 0.5 is used in the analyses, although Dobry et al. (1997) examined the scaling factor for k_h for various L_U in pile loading tests in a centrifuge and concluded that α=1. Since the larger α makes k_h smaller at the same L_U, this may result in better results.

Use of excess pore water pressures measured at the array far from the pile has perhaps caused error in the scaling factor determination. Fig. 13 plots calculated bending moment distribution of the pile and displacement profiles of soil and pile for Case 2-6 using the excess pore water pressures measured at the array near the pile (P6 to P10 in Fig. 6). The excess pore water pressures measured at the array near the pile were larger than those at the array far from the pile at the target time and the calculated results are more comparable to the measured ones.

If one wants to fit the calculated results to the observed, either way, i.e., review of α or L_U, can be chosen. Accumulation of high quality test and field measurement data is required for the better determination of α and L_U.

4.4 Effects of soil deformation on pile response

Figure 14 demonstrates the importance of soil deformation on the pile response. This figure plots the calculated bending moment distributions of the pile subjected to (1) the footing inertial force only, or (2) that plus the soil movement, for all the cases. The maximum bending moment distribution calculated only with the pile head loading is well below that with the soil movement, and shape of the obtained bending moment distribution for that condition is not similar to that observed, as expected. These results ensure importance of the soil movement consideration in the pile response calculation.

5. SUMMARY

This paper demonstrates application of the beam on Winkler foundation approach to a pile foundation in liquefying soil by comparing the analysis results with centrifuge model test data. Non-linear Winkler (*p-y*) springs that model lateral soil-pile interaction play a key role in this kind of analysis. Firstly, direct measurement of the lateral resistance of a pile at the non-liquefiable surface layer during an earthquake was attempted in centrifuge model tests. Based on this test results, the normalised *p-y* curve for the surface layer is modelled as an equivalent linear Winkler spring.

A series of centrifuge model tests on a pile group in the liquefying soil is analysed using the above-mentioned spring for the surface layer and that recommended in the specifications for highway bridges (JRA 2002) for the other layers. Analysis results ensure importance of the soil movement consideration in the pile response calculation. Appropriate modelling of the Winkler spring and its scaling factor considering the excess pore water pressure ratio in non-liquefiable layers allow us to evaluate pile performance in the liquefied soil accurately.

References

Architectural Institute of Japan. 2001. Recommendations for design of building foundations, 485pp. (in Japanese).

Hiro-oka, A., Okamura, M., Takemura, J. & Kimura, T. 1995. Dynamic behaviors of compacted sands surrounded by liquefied loose sand, *Proceedings of the 1st International Conference on Earthquake Geotechnical Engneering*, Vol. 2, 681--686.

Dobry, R., Taboada, V. & Liu, L. 1997. Centrifuge modelling of liquefaction effects during earthquake, *Proceedings of the 1st International Conference on Earthquake Geotechnical Engneering*, Vol. 3, 1291--1324.

Japan Road Association. 2002. Specifications for road bridges, Part V, Seismic Design, 333pp.

Japan Society of Civil Engineers. 2000. Earthquake Resistant Design Codes in Japan.

Kobayashi, H. & Tamura, K. 2002. Acceleration response spectra for design of road bridges on liquefiable soil, *Proceedings of 5th Symposium on Ductility Design Method for Bridges*, 113--116 (in Japanese).

Ono, K., Tamura, K., Okamura, M. & Tanimoto, S. 2003. Experimental study on bridge pile subjected to large soil deformation in liquefying soils, *Proceedings of 6th Symposium on Ductility Design Method for Bridges*, 257--262 (in Japanese).

Railway Technical Research Institute. 1997. Seismic design for foundations, *Foundation design codes for railway structures*, 467pp (in Japanese).

Sakemi, T., Tanaka, M., Higuchi, Y., Kawasaki, K. & Nagura, K. 1995. Permeability of pore fluids in the centrifuge field, *Proceedings of the 10th Asian Regional Conference on Soil Mechanics and Foundation Engineering*, 481--484.

Sato, N., Tamura, K., Azuma, T. & Kobayashi, H. 2001. Experimental study on pile response in liquefying soil, Proceedings of the 26th JSCE Earthquake Engineering Symposium, Vol.1, 849--852 (in Japanese).

Tokimatsu, K. & Asaka, Y. 1998. Effects of liquefaction-induced ground displacements on pile performance in the 1995 Hyogoken-Nambu Earthquake, *Soils and Foundations, Special Issue on Geotechnical Aspects of the Jan. 17 1995 Hyogoken-Nambu Earthquake*, No. 2, 163--177.

Tokimatsu, K. 2003. Behavior and Design of Pile Foundations Subjected to Earthquakes, *Proceedings of the 12th Asian Regional Conference on Soil Mechanics and Geotechnical Engineering, Singapore*, Vol.2.

Table 1: Test conditions for direct *p-y* curves measurement in shaking table test (in prototype scale)

Case No.	Thickness of liquefiable layer (m)	Thickness of non-liquefiable surface layer (m)	Relative density of sand (%)	Maximum input motion acceleration (G)
Case 1-1	2.50	5.00	41.8	0.24
Case 1-2	2.50	5.00	28.8	0.24
Case 1-3	4.50	3.75	27.9	0.45

Table 2: Parameters for subgrade reaction coefficient in non-liquefiable surface layer

Case No.	Relative density of sand (%)	Parameter A	Parameter B
Case 1-1	41.8	16	0.7
Case 1-2	28.8	10	0.7
Case 1-3	27.9	7.9	0.7

Table 3: Test conditions for centrifuge model tests on pile group in liquefying soil (in prototype scale)

Case No.	Thickness of liquefiable layer (m)	Thickness of surface layer (m)
Case 2-3	9.45	0.00
Case 2-4	6.30	3.15
Case 2-6	3.15	6.30

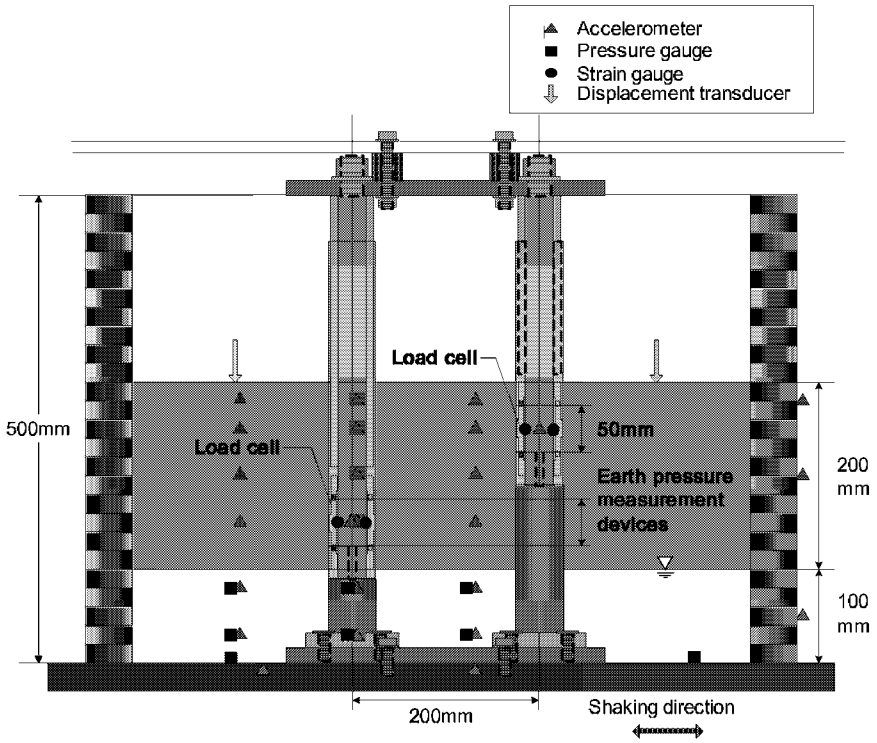

Figure 1: Model setup for *p-y* relation measurement centrifuge tests.

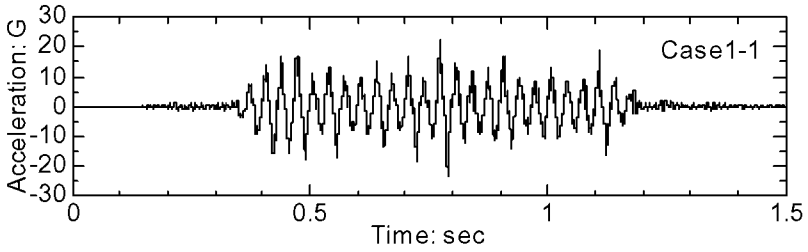

Figure 2: Typical input motion for *p-y* relation measurement (in model scale).

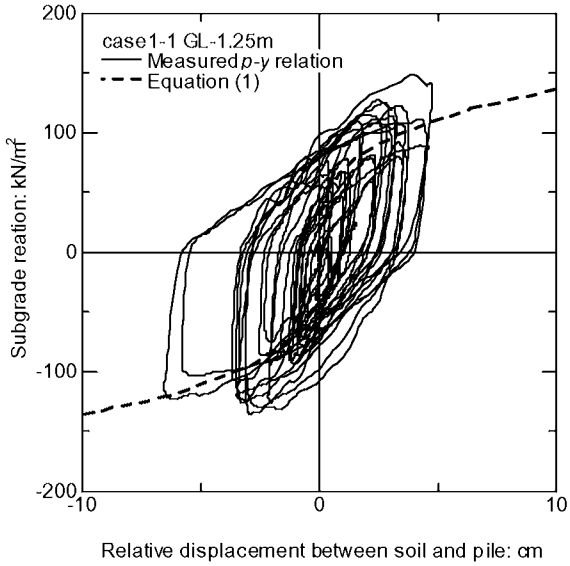

Figure 3: Typical *p-y* curve (Case 1-1).

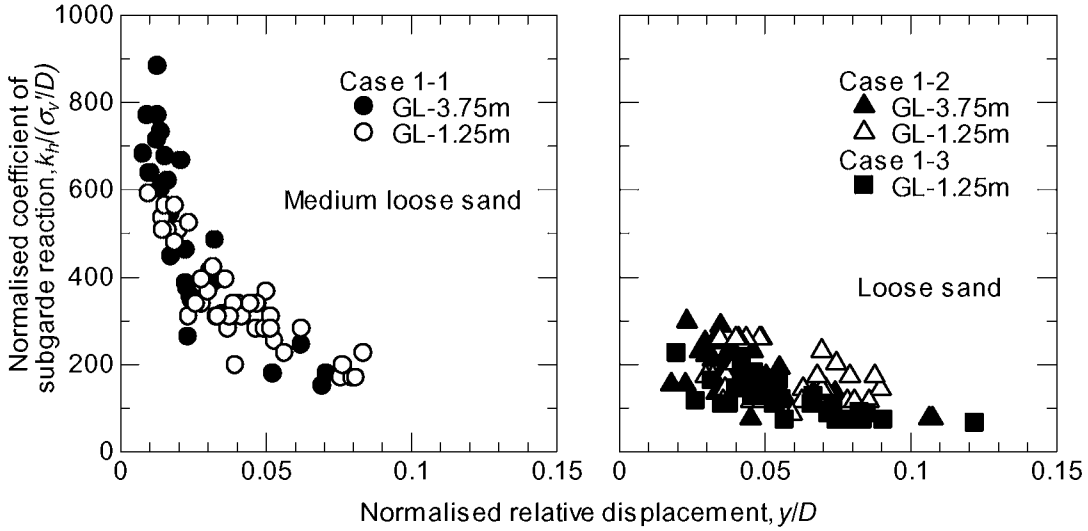

Figure 4: Normalised subgrade reaction coefficient against normalised soil-pile relative displacement.

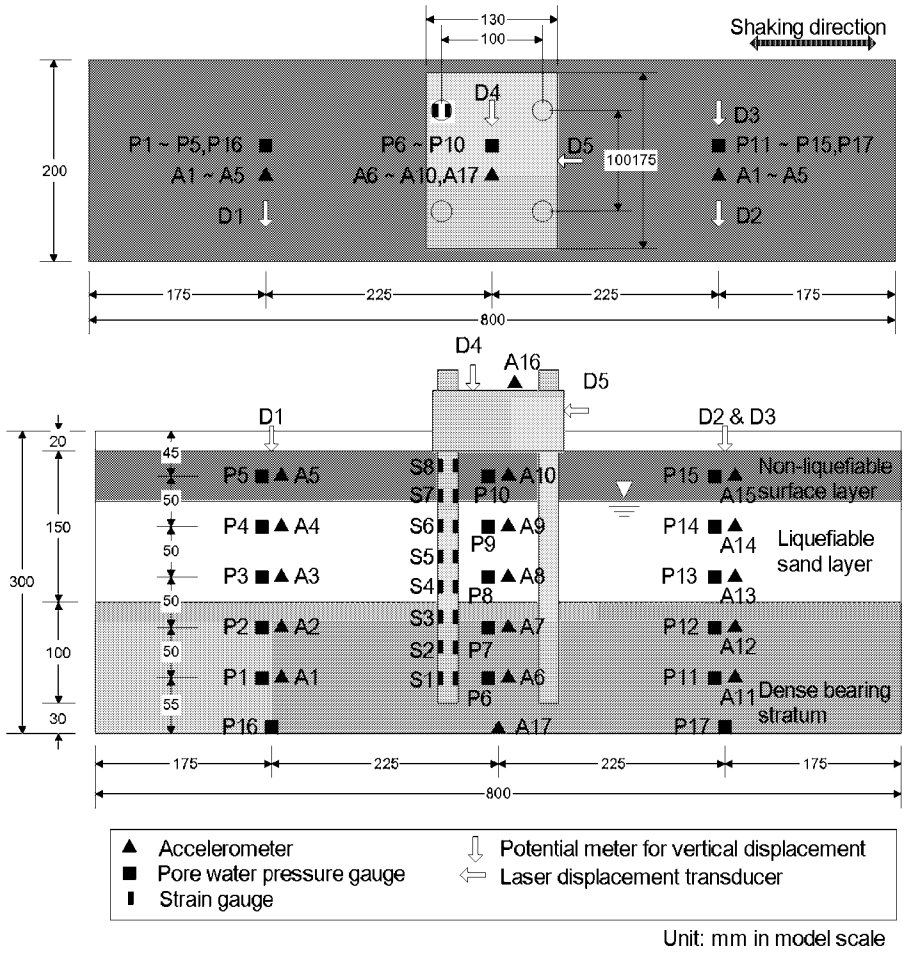

Figure 5: Model setup for shaking table tests on pile group in liquefying soil.

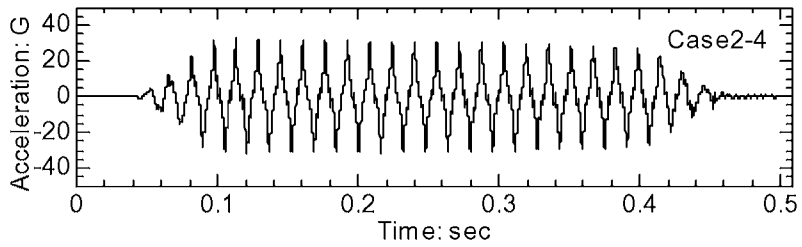

Figure 6: Typical input motion for shaking table test (in model scale).

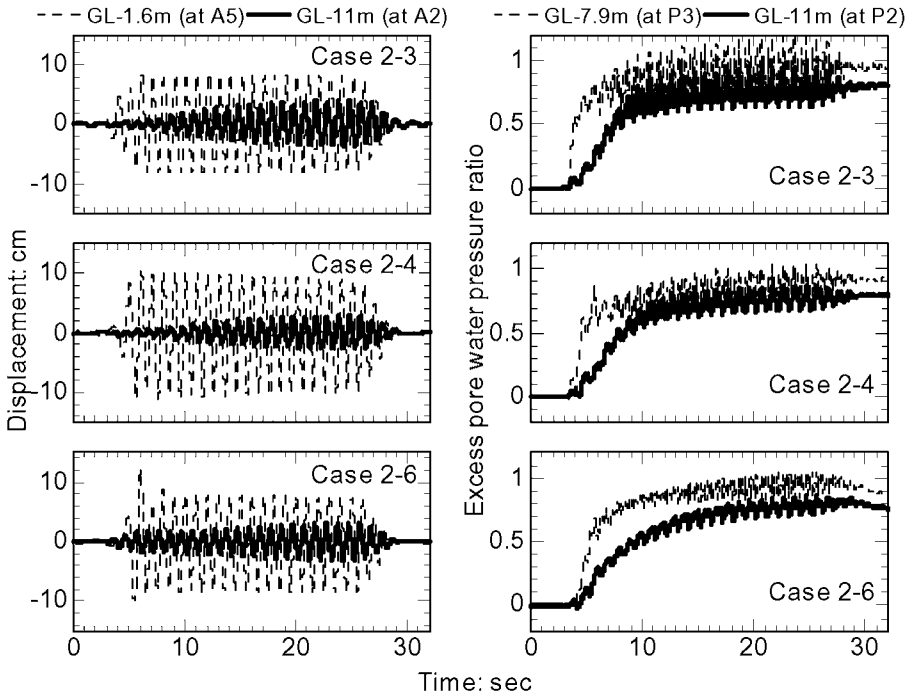

Figure 7: Time evolutions of relative horizontal ground displacement excess pore water pressure.

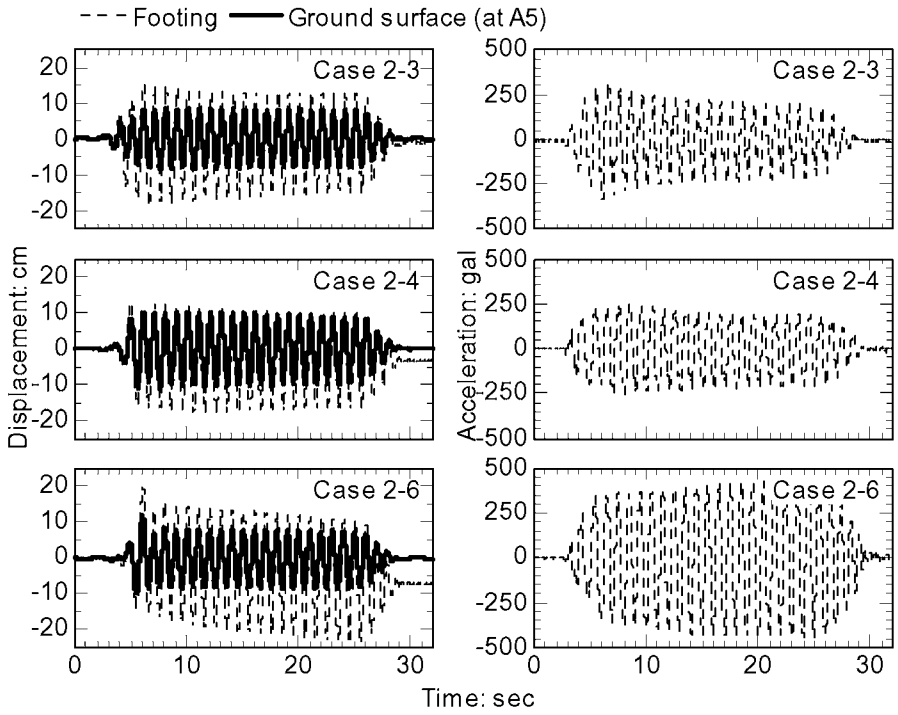

Figure 8: Time evolutions of relative horizontal displacement of ground surface and footing and acceleration of footing.

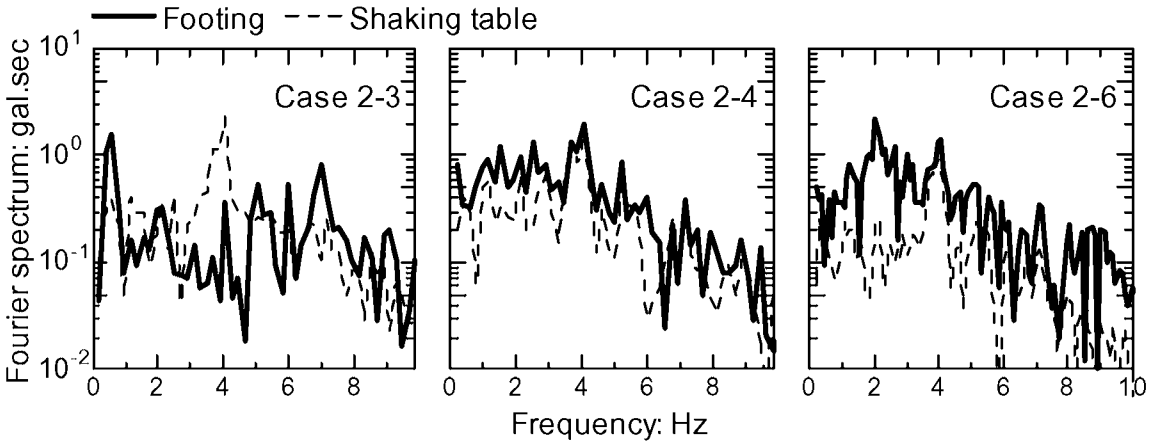

Figure 9: Fourier spectra of free vibration of footing and shaking table just after shaking.

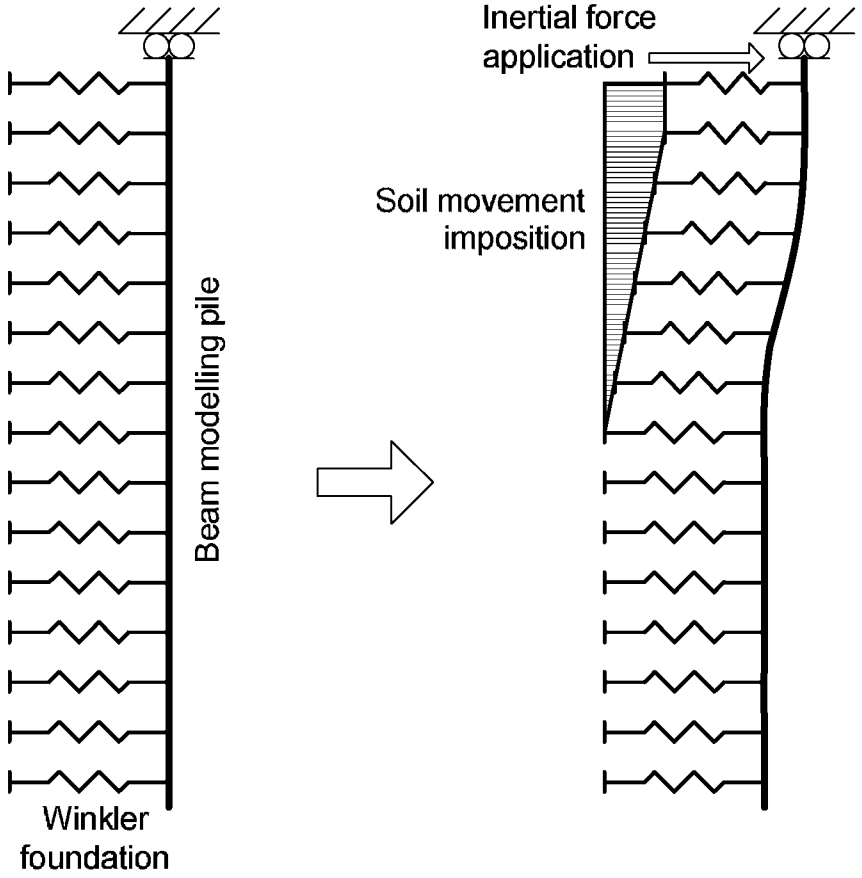

Figure 10: Analytical model used.

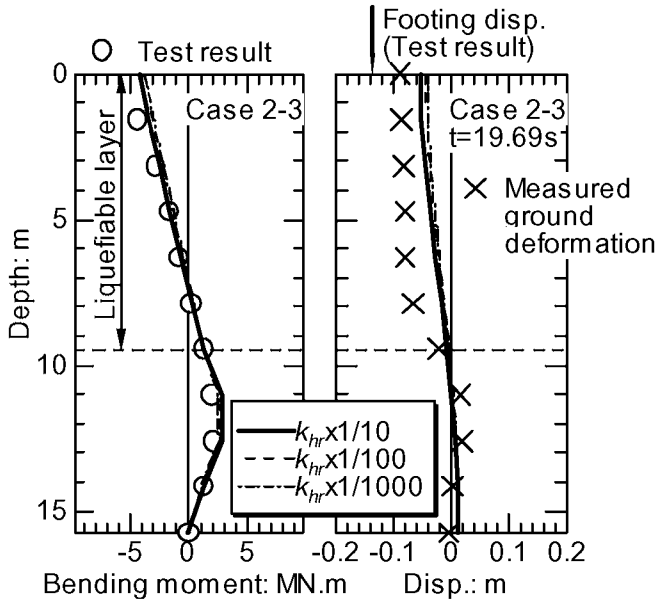

Figure 11: Pile bending moment distributions and displacement profiles (Case 2-3).

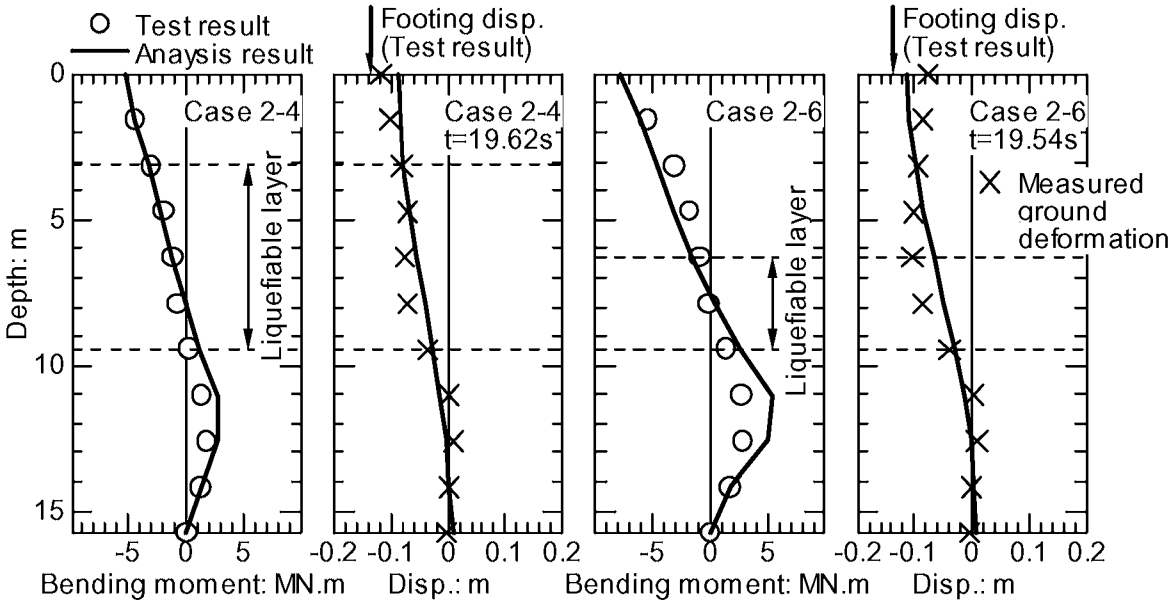

Figure 12: Pile bending moment distributions and displacement profiles (Cases 2-4 & 2-6).

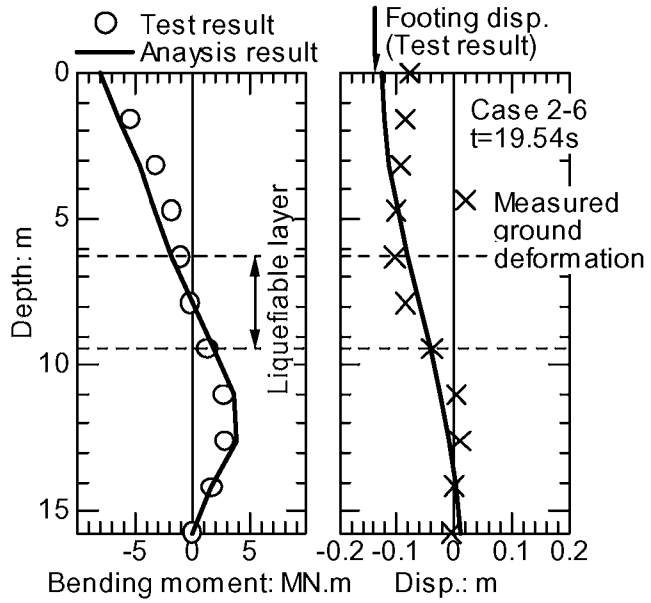

Figure 13: Pile bending moment distributions and displacement profiles with excess pore water pressure measured around pile (Case 2-6).

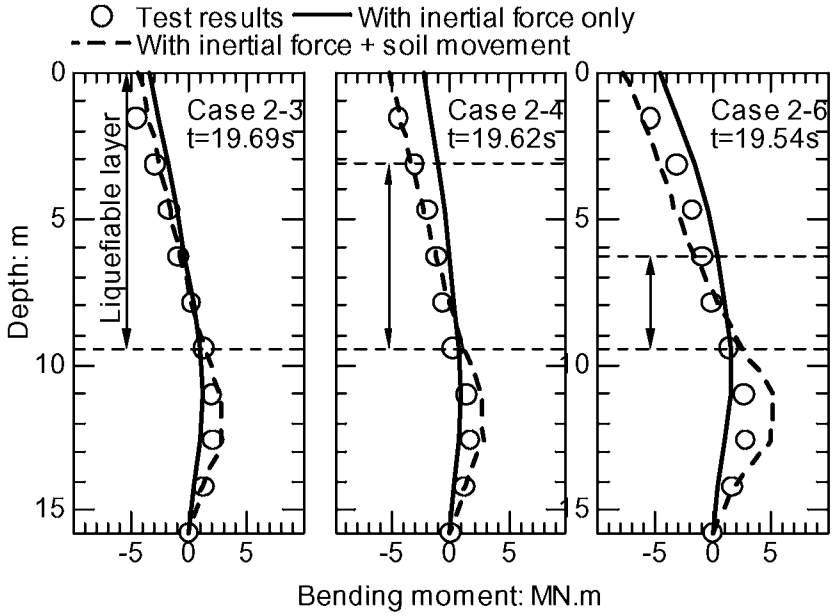

Figure 14: Bending moment distributions of pile with and without inertial force acting on pile top cap.